

# The Life and Times of AMBER: The VLTI's Astronomical Multi-BEam combineR

Willem-Jan de Wit<sup>1</sup>  
 Markus Wittkowski<sup>1</sup>  
 Frederik Rantakyro<sup>2</sup>  
 Markus Schöller<sup>1</sup>  
 Antoine Mérand<sup>1</sup>  
 Romain G. Petrov<sup>3</sup>  
 Gerd Weigelt<sup>4</sup>  
 Fabien Malbet<sup>5</sup>  
 Fabrizio Massi<sup>6</sup>  
 Stefan Kraus<sup>7</sup>  
 Keiichi Ohnaka<sup>8</sup>  
 Florentin Millour<sup>3</sup>  
 Stéphane Lagarde<sup>3</sup>  
 Xavier Haubois<sup>1</sup>  
 Pierre Bourget<sup>1</sup>  
 Isabelle Percheron<sup>1</sup>  
 Jean-Philippe Berger<sup>5</sup>  
 Andrea Richichi<sup>6</sup>

<sup>1</sup> ESO

<sup>2</sup> Gemini Observatory

<sup>3</sup> Université Côte d'Azur, France

<sup>4</sup> Max-Planck-Institut für Radioastronomie, Bonn, Germany

<sup>5</sup> Institut de Planétologie et d'Astrophysique de Grenoble, France

<sup>6</sup> INAF-Osservatorio Astrofisico di Arcetri, Italy

<sup>7</sup> University of Exeter, UK

<sup>8</sup> Universidad Católica del Norte, Chile

The sharpest images on Paranal are produced by the beam-combining instruments of the Very Large Telescope Interferometer (VLTI). Currently, the VLTI is close to completing a transitional period, moving away from the first generation of instruments (AMBER, MIDI) and offering new instruments and subsystems to the community. In this article, we report on the life and achievements of the recently decommissioned, near-infrared beam combiner instrument AMBER, the most prolific optical interferometric instrument to date.

## AMBER, a three-telescope combiner

AMBER was one of three ambitious, general-user, interferometric instruments proposed in 1997 for implementation on the VLTI at Paranal (Paresce et al., 1996), following the recommendations of the Interferometry Science Advisory Committee to ESO. In optical interferometry, new

instruments are scientifically inaugurated via their “first fringes”, which is the interferometric equivalent of “first light”. By the early 2000s, the integration of ESO's interferometer into the VLT architecture was on track.

The first Paranal interference fringes were produced by the VLT Interferometer Commissioning Instrument (VINCI) and MID-infrared Interferometric instrument (MIDI), instruments that combined the light from two telescopes. VINCI's purpose was to commission the interferometer's infrastructure. MIDI, on the other hand, was the first scientific instrument in operation using the VLTI in conjunction with the 8.2-metre Unit Telescopes (UTs). The second scientific VLTI instrument to arrive on Paranal was AMBER. It had been conceived as a potential sea change in optical interferometry, exploiting the idea of spectro-interferometry — obtaining spatial information on milliarcsecond scales at high spectral resolution. It comprised three spectral settings, including a high spectral resolution of  $R = 12\,000$ , and was foreseen to work at a high sensitivity and with high visibility accuracy in three infrared atmospheric windows ( $J$ -,  $H$ -, and  $K$ -bands). Yet, arguably its most important asset was the capacity to combine the light beams from three separate telescopes at long baselines, a novelty in long-baseline optical interferometry which allowed milliarcsecond-resolution images to be synthesised at high spectral resolution.

The consortium of four institutes driving the AMBER project consisted of the Observatoire de la Côte d'Azur (OCA: the Principal Investigator institute) in Nice, the Laboratoire d'Astrophysique de l'Observatoire de Grenoble (LAOG at the time, now called IPAG), the Max-Planck-Institut für Radioastronomie (MPIfR) in Bonn, and the Osservatorio Astrofisico di Arcetri in Florence. It built on the European expertise of designing two-telescope combiners capable of exploiting spectro-interferometry and the usage of single-mode fibres. Conceptually, to advance from two-telescope to three-telescope combiners may seem a small step, but scientifically it constituted a leap forward.

The crucial consideration is to provide access to the observational quantity

called the closure phase. The absolute phase of incoming light waves is scrambled by atmospheric turbulence, resulting in distortion over a pupil and global phase shifts between the apertures in the array (called the piston). The degree and frequency of the scrambling increases towards shorter wavelengths. As a result, the coherence time of the incoming wave ranges from a few milliseconds to (at best) some tens of milliseconds in the optical regime. There is no way to beat the turbulence and recover the phase without additional aids. When combining three telescopes arranged in a closed triangle one can retrieve a new observable by adding the phases. This resulting closure phase is invariant to atmospheric perturbations, as the atmospheric phase noise terms from each individual telescope cancel out. The technique was first applied in radio interferometry. Physically, the closure phase quantity is a proxy for the degree of asymmetry in the science target. Closure phase information is a pre-requisite to reconstructing images from interferometric observables (for example, Jennison, 1958; Baldwin et al., 1996) and AMBER was the first instrument at the VLTI to deliver it.

AMBER produced clear first fringes of the star  $\theta$  Centauri on the night of 20 March 2004 using two telescopes at a baseline of 64 metres, marking a milestone after seven years of work. The instrument was offered to the community for the first time in observing period 76 (starting October 2005), fed by the large apertures of the UTs.

## Optical principle and early years

AMBER's design corresponds broadly to an optical configuration similar to the one that creates fringe patterns in a Young's interference experiment, i.e., overlapping images coming from multiple telescopes (or beams). Most importantly, before the light is recombined, each light beam is guided through a single-mode fibre. A single-mode fibre acts as a spatial filter and rejects the distorted part of the wavefront, leading to a flattened exit wavefront. The phase fluctuations are traded against fast intensity fluctuations (which are recorded) and a global piston (which is measured from the slope of

the dispersed fringes). Hence, AMBER implements three photometric channels for the simultaneous monitoring of the beam intensity for each telescope beam. Recombination, and with it the production of fringe patterns, is done after forming three exit pupils. The exit pupils are physically placed in a non-redundant manner such that the set of three contained spatial frequencies in the final interferometric image are fixed (i.e., non-homothetic) but different and identifiable. The four beams — three intensity monitoring beams and the one interferometric beam containing all the information for the three baselines — are then spectrally dispersed before detection (Petrov et al., 2007).

The integration of AMBER operations into the complex VLTI and telescope architecture was an iterative process (see Mérand et al., 2014). For example, operations began with the UTs equipped with the Multiple Application Curvature Adaptive Optics (MACAO) guiding systems, before the arrival of the versatile Auxiliary Telescopes (ATs). The ATs were commissioned in the summer of 2006 and first offered in April 2007 with a limited set of baselines. On the VLTI side, the injection of the light into the instrument's single-mode fibres was optimised by controlling the tunnel tip-tilt inside the VLTI laboratory using the InfraRed Image Sensor (IRIS). This sensing sub-system was operated from 2006 onwards but using the telescopic XY table as a corrective system. As a result, it operated at a sub-optimal slow rate of about 1 Hz, but it was nonetheless quickly seen as a mandatory prerequisite for improved beam injection.

After the first couple of years of operation it became clear that AMBER was not fulfilling all of its potential on the VLTI. As the first VLTI instrument to possess high spectral resolution, and therefore to require longer integration times, it demanded much more from the VLTI infrastructure than its predecessors. Flux injection and phase stability had to be significantly improved. The observation overheads were large, the quality of the high-spectral-resolution data was degraded, and the sensitivity was limited. These problems and others were tackled thanks to increased efforts from the

AMBER consortium in 2007–2008, and through the continuous improvement of the VLTI infrastructure.

A report analysing the accuracy in absolute visibility, closure phase and differential phase identified critical software and hardware improvements required by AMBER (Malbet et al., 2008). The main modifications in AMBER were the replacement of its polarisation filters which were responsible for parasitic Fabry-Perot fringes in all the spectro-interferometric measurements, and improvements in its operation and maintainability. On the VLTI, after a significant improvement in the delay line models, a continuous effort resulted in the progressive reduction of the vibrations in the coudé trains of the UTs. A decisive factor was the implementation of a faster loop to counter the flux dropouts seen in the instrument — a higher correction rate was made possible by offloading the measured IRIS tip-tilt to the feeding optics of AMBER. AMBER's performance could be further improved thanks to the arrival of the Fringe-tracking Instrument of Nice and Torino (FINITO) (Haguenaue et al., 2008).

### Arrival of FINITO

The art of fringe tracking was introduced into AMBER operations for the Period 80 call for proposals in October 2007. The purpose of fringe tracking is to nullify the fringe movement caused by atmospheric turbulence which blurs the contrast of the fringes. With FINITO, longer detector integration times could now be employed. Longer integration of fringe patterns allows the observation of targets at a higher spectral resolution, or of fainter sources, or allows a lower intrinsic fringe contrast to be measured. Additionally, longer detector integration times also allow the full detector to be read out, increasing the spectral range covered by the observations. Fringe tracking was implemented in the VLTI by means of the separate instrument FINITO (Gai et al., 2004). Its purpose was to measure the broad-band fringe jitter at kHz frequency in the *H*-band. The FINITO signal was processed and injected back into the VLTI in real time via the Reflective Memory Network architecture. As of Period 83

(April 2009) standard AMBER operations for medium and high spectral resolution were done in conjunction and simultaneously with FINITO. Since 2011, the FINITO data have been delivered alongside the AMBER ones for optimised data reduction and post-processing purposes. With the advent of GRAVITY fringe tracking has become an integral part of the science observations and the data from the fringe tracker are used in the data reduction process.

Continual enhancements of AMBER and the VLTI resulted in steady improvements of the limiting magnitude and operational efficiency. AMBER's self-coherencing was introduced in April 2012 for the low-resolution setup. This mode allowed automatic real-time fringe centring at a relatively low cadence when fringe tracking with FINITO was not possible (for example, because of seeing conditions or low source flux). The instrument intervention performed at the end of 2012 changed the spectrograph beamsplitter that caused internal reflections; this resulted in almost a 30% improvement in throughput in the interferometric channel. Better polarisation control, by means of birefringent lithium niobate (LiNbO<sub>3</sub>) plates, was introduced in October 2014, following an earlier implementation in the Precision Integrated Optics Near-infrared Imaging Experiment (PIONIER). Such plates allow the equalisation of the phase difference between the two polarisation stages and add them incoherently, improving the sensitivity by a factor of nearly two. At the same time the observing efficiency improved dramatically by a factor of three since the start of operations, resulting in much shortened execution times of 20 minutes per Observation Block (OB), down from one hour.

### Science delivered

ESO's AMBER and VLTI infrastructure delivers observable quantities that reveal the wavelength-dependent structure and geometry of astrophysical sources at a very high angular resolution: indeed, the best available from any of the ESO instruments. At the wavelength of operation, AMBER can reach angular resolutions of the order of 1 milliarcsecond. The differential phase accuracy allowed photocentre

displacements as small as 10 micro-arcseconds to be measured, for example, in the alignment between the stellar rotation axis and the orbits in the Fomalhaut debris disc system (Le Bouquin et al., 2009). The superb angular resolution allows breakthrough science by delving into spatially unexplored regions on stellar surfaces, in the circumstellar environment of young and evolved stars, and around the active nuclei of galaxies.

ESO's Telescope Bibliography telbib provides the following statistics for the science legacy of AMBER. Up to October 2018, AMBER data contributed to 153 peer reviewed science papers. This number nearly equals the total number of science papers produced with data from MIDI, which was decommissioned in March 2015. The number of papers makes these two instruments the most productive in terms of science papers produced using data from a long-baseline optical interferometry facility. Over the period 2015–2017, about ten papers per year were published with AMBER data; given that telbib publication analyses estimate an average lag time between the execution of a programme and the publication of a paper of approximately 5.4 years for 50% of the data, it is not unreasonable to expect a few tens of peer-reviewed AMBER papers to see the light of day in the coming years.

Regarding instrument modes, the relative demand for the various AMBER spectral settings varied substantially, with the low-resolution and medium-resolution setups vying for dominance. The low-resolution time requested strongly dominated up to Period 88, with over 80% of the demand between Periods 79 and 82. After Period 88, the medium-resolution settings (*H*- and *K*-band) became more popular, leading to approximately 60% of the time requested after Period 94. The high-spectral-resolution setting request fluctuated around 20% of the total time after Period 82, coinciding with the introduction of FINITO to VLTI and UT operations.

The topics of the science papers deal almost exclusively with stellar evolution, in particular star formation and young stars, late evolutionary stages of intermediate- and low-mass stars (for example, asymp-

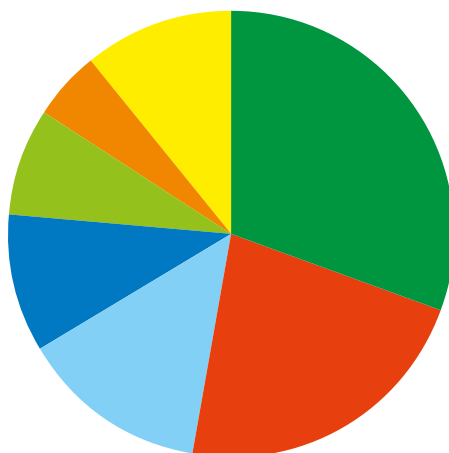


Figure 1. Distribution (in percent) of science topics of 153 peer-reviewed articles based on AMBER data. The large majority of papers (31%) are centred on young stars, in particular the structures that allow the growth of the star (for example, accretion disc, disc-wind, jet formation).

totic giant branch [AGB] stars) and high-mass stars. Their fractional contribution by sub-category is presented in Figure 1, and we highlight some of these science cases in the next section.

The sub-topics cover a wide range of science cases, from the evolution of cool evolved stars, concentrating on circum-binary discs of post-AGB stars and supergiant B[e] stars, the inner wind regions in neutral and ionised gas of post-red supergiants and unstable hypergiants, and the nebulae of Wolf-Rayet stars.

One example of exploiting aperture synthesis imaging to better understand evolved high-mass stars is the image of the well-known luminous eruptive star  $\eta$  Carinae, shown in Figure 2. It is one of

the first direct images of the innermost part of the wind-wind collision zone, a key feature of the observed erratic behaviour of this object. A series of papers reported investigations of the evolution of novae and their environment (for example, Chesneau et al., 2007) and the detection and characterisation of binaries and higher order stellar multiples. AMBER also observed the nucleus of the Seyfert galaxy NGC 3783, deriving a ring radius for the toroidal dust distribution of 0.74 milliarcseconds (Weigelt et al., 2012).

The most cited AMBER paper to date analyses the measured radii of seven low- and very-low-mass stars, finding agreement between the observed radii and the predictions of stellar evolutionary models for magnetically active low-mass stars (Demory et al., 2009; Figure 3).

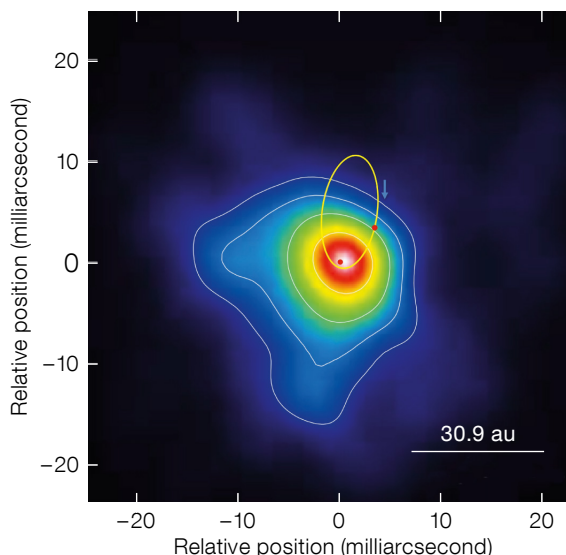


Figure 2. Aperture synthesis image of  $\eta$  Carinae in the Brackett  $\gamma$  HI transition at a radial velocity of  $-277 \text{ km s}^{-1}$ . The image shows both the dense stellar wind surrounding the primary star (red, yellow, and green regions) and the fan-shaped wind-wind collision zone (blue). The image field of view is  $50 \times 50$  milliarcseconds. Overlaid is a sketch of the orbit of the secondary star (adapted from Weigelt et al., 2016).

We note that, after the first successful science observations, an issue of *Astronomy & Astrophysics* (Volume 464, No. 1, March 11 2007) was dedicated to the first results from AMBER, including the instrument description and the first astrophysical results.

### The physics of young stars

AMBER's scientific contributions in the field of young stars are impressive. It is clear that stars accrete mass from their environments, as revealed, for example, by the spectroscopic and photometric activity of young objects. How the process of accretion actually manifests remains less clear. AMBER contributed to revealing the geometry of the accretion environment in young stars.

Notably, an aperture synthesis image created by Kraus et al. (2010) showed a disc surrounding a young,  $20 M_{\odot}$  star at a spatial resolution of 2.4 milliarcseconds (see Figure 4). It demonstrates the inevitability of disc formation for mass accretion to proceed, even in high-mass luminous stars. How the disc is shaped and its structure closer to the stellar surface are revealed in the 1500 visibility measurements reported by Benisty et al. (2010) where the inner few astronomical units dominate the emission in the *H*- and *K*-bands. These hot disc regions give rise to large-scale ionised winds (for example, Malbet et al., 2007), or they diminish to very compact ionised regions possibly identifying the actual process of depositing material on the star's surface or the jet launching environment (Kraus et al., 2008). The brightness, relative proximity and complexity of various physical processes operating during the accretion process make bright young stars extremely suitable targets for spectro-interferometry. These and other high-angular-resolution findings formed the rationale for the second conference dedicated to intermediate-mass pre-main-sequence stars organised in Vitacura in 2014 (de Wit et al., 2014).

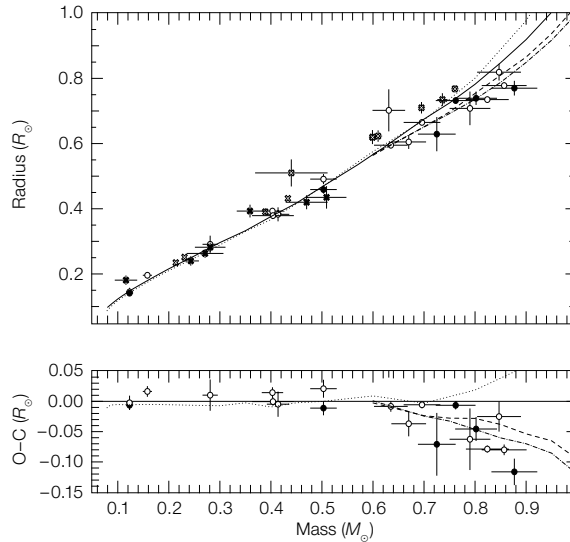


**Figure 3.** The mass-radius relationship for M- and K-type dwarfs, for which radii have been obtained via direct measurements with AMBER and VINCI (filled circles). Other long-baseline observations are overplotted (solid, dashed and dotted lines) in open circles. Evolutionary predictions are for an age of 5 Gyr and different values for the convective overshoot parameter (adapted from Demory et al., 2009).

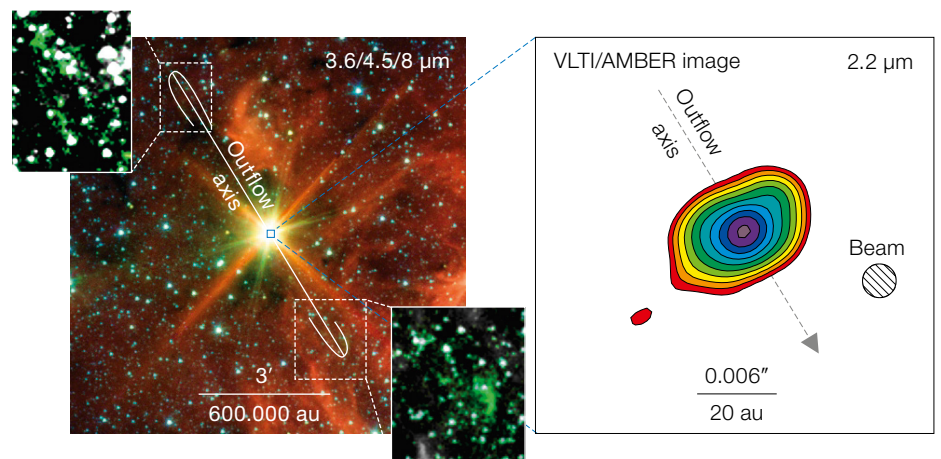


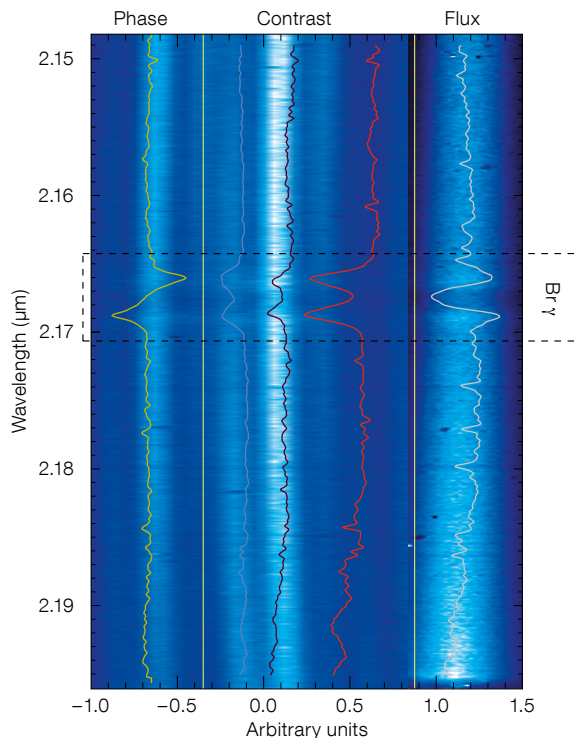
**Figure 4 (below).** Left: Mid-infrared Spitzer composite image ( $3 \times 3$  arcminutes) of the surroundings of the  $20 M_{\odot}$  young star IRAS+13481-6124, revealing the outflow from the star as indicated. Right: AMBER aperture synthesis image zooming in on the accretion disc. Modelling shows that the disc has a dust-free region inside 9.5 astronomical units from the star. The structure is oriented perpendicular to the outflow direction (adapted from Kraus et al., 2010).

### Fast rotating stars

The fastest rotating stars reaching critical velocity (at which a star breaks up) are the 6 to  $15 M_{\odot}$  stars. Indeed, the early B-type stars, as a general group, display the fastest rotation of all stars. Such rapid rotation can be assessed by either measuring the shape of the star (via visibilities), or exploiting Doppler effects in a spectral transition resulting from the stellar rotation. In the latter case, one exploits the fact that the photocentre of the stellar surface in the approaching part of the spectral line profile is different from that in the receding part. AMBER allows this effect to be measured as it provides access to the phase changes relative to each spectral bin.

Domiciano de Souza et al. (2012) infer the equatorial radius, the inclination angle and an equatorial rotational velocity of  $298 \pm 9$  km/s for the rapidly rotating B star Achernar using this technique (see Figure 5). Owing to this fast rotation, the classical Be stars are capable of launching stellar material into a circumstellar disc. With the help of AMBER data, direct evidence was obtained that these discs are in clear Keplerian rotation, a suggestion that dates back to their discovery in 1866 (Meilland et al., 2007). Further investigation shows that this type of disc is generally expanding, and forms a one-armed spiral density pattern that precesses with a period of a few years (Carciofi et al., 2009).

**Figure 5.** A popular transition is the Brackett  $\gamma$  H I atomic line at 2.17  $\mu\text{m}$ . For the last AMBER fringes, the rapidly rotating star Achernar ( $\alpha$ Eridani) was targeted. Its rotation ( $\sim 90\%$  of the critical velocity) causes its equatorial diameter to be about 35% larger than its polar diameter. The blue background image shows the interferometric beam with fringes (stretching from  $x = -1.0$  to 0.9), and overlaid are the extracted contrast for the three baselines and the closure phase. The image also shows one photometric beam ( $x = 0.9$  to 1.5), and overlaid is Achernar's flux spectrum. AMBER observations are sensitive to the disc rotating in the Brackett  $\gamma$  H I transition, characterised by a decrease in contrast and the opposite phase signature.



### Cool evolved stars and their further evolution

The AMBER instrument made significant contributions to the study of cool evolved stars and their further evolution throughout its operational lifetime. In total, about a quarter of the papers based on AMBER data fall into this scientific category.

Cool evolved stars comprise AGB and red supergiant (RSG) stars, which are located on the Hertzsprung-Russell-Diagram (HRD) at effective temperatures between about 2500 and 4500 K. They cover a large range of luminosities depending on their initial mass, where AGB stars are low- to intermediate-mass stars, and RSGs their massive and high-luminosity counterparts. Owing to the low temperatures of AGB and RSG stars, molecules and dust can form in their atmospheres, and they are subsequently expelled into the interstellar medium via a stellar wind with similar mass-loss rates found in AGBs and RSGs. When AGB stars have lost a significant fraction of their mass, they evolve again toward higher effective temperatures, and via a post-AGB phase they transition to planetary nebulae. RSG stars explode as core-collapse supernovae

or transition to hotter Wolf-Rayet stars, depending on their mass.

Previous interferometric observations of cool evolved stars were usually made via broad filters or sequentially in a few narrow bandpasses, the latter a time-consuming technique. AMBER has been unique in providing detailed measurements of individual lines, in particular the individual CO first overtone lines near 2.3  $\mu\text{m}$ , with a high spectral resolution of  $R \sim 12\,000$  (for example, Ohnaka et al., 2011), or measurements across the full  $K$ -band with the medium spectral resolution of  $R \sim 1500$  (for example, Wittkowski et al., 2008). Cool evolved stars appear to be extended in bandpasses that are dominated by molecular layers, and much more compact in near-continuum bands. Observing spectral channels across the  $K$ -band at once has been an essential tool to constrain dynamic model atmospheres. High-spectral-resolution studies of CO first overtone lines showed extended CO layers in detail as well as their vigorous, inhomogeneous large-scale motions.

For Mira-variable AGB stars, it has been shown that pulsation and convection can lead to strongly extended molecular

atmospheres, where the temperature is cool enough for dust to form. AMBER observations of these stars have been shown to be largely consistent with dynamic model atmospheres at individual phases, and have confirmed time variability of molecular extensions on time scales of weeks to months.

For RSGs, it has been speculated that the same processes may explain their mass loss as well. However, AMBER observations of RSGs showed extensions that are larger than expected based on current dynamic model atmospheres. Direct comparisons of AMBER data with 1D and 3D dynamic model atmospheres showed that current models of RSGs based on pulsation and convection alone cannot explain observed extensions of RSG atmospheres, and cannot explain how the atmosphere is extended to radii where dust can form (for example, Arroyo-Torres et al., 2015). This points to missing physical processes in current RSG dynamic models — an unsolved problem that is a heritage of AMBER and that is due to be investigated further by the next-generation interferometric instruments. AMBER has also provided observations of non-Mira red giants which are partly consistent with hydrostatic models and partly show discrepancies with models similar to RSGs. AMBER has provided image reconstructions of both the extended atmospheres of AGB stars (for example, Le Bouquin et al., 2009) and RSGs (for example, Ohnaka, Weigelt & Hofmann, 2017; see Figure 6).

### Conclusion

On the night of 3 September 2018, the interferometric instrument AMBER observed its last fringes. After serving the European astronomy community for over thirteen years, the instrument was decommissioned during the course of the interventions in the VLTI laboratory that were necessitated by the arrival of the adaptive optics system for the ATs (NAOMI) and the Multi AperTure mid-Infrared SpectroScopic Experiment (MATISSE). AMBER operations encouraged the development of the FINITO fringe-tracker to beat the atmosphere's phase disturbance, which enabled longer detector integration times. With the

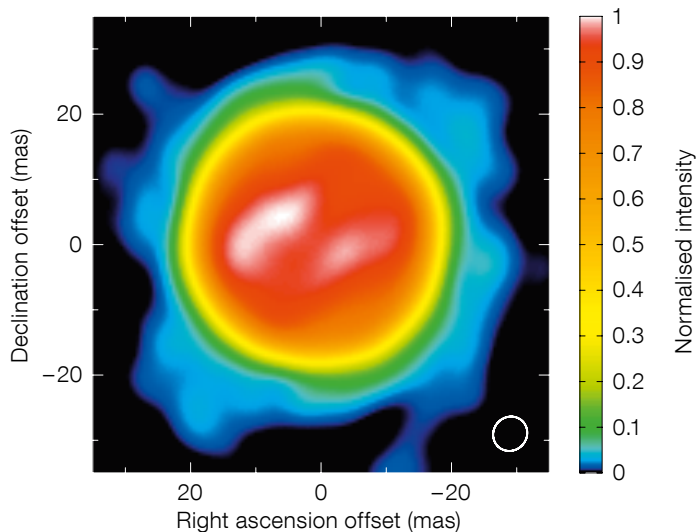


**Figure 6.** Velocity-resolved aperture synthesis imaging of the red supergiant Antares. This monochromatic image was obtained at the centre of the CO transition at 2.30665  $\mu\text{m}$ . AMBER's high spatial and spectral resolution allowed the observations to measure the "vigorous" motion above the complex red supergiant photosphere (adapted from Ohnaka, Weigelt & Hofmann, 2017).

decommissioning of both AMBER and FINITO, the VLT Interferometer bids farewell to the era of the first generation of interferometric instruments at Paranal. The new era of VLTI operations is marked by routinely making use of the four-telescope combiner instruments, GRAVITY, PIONIER, and the latest addition, MATISSE.

In many respects, AMBER represented a breakthrough in optical interferometry. At Paranal, it was the first instrument to combine the beams of three telescopes, providing access to the all-important closure phase, without which it is not possible to reconstruct images of celestial objects from interferometric observations. As such, and in addition to the visibility and phase studies, AMBER has delivered a great number of images at milliarcsecond scales, providing new insights into astrophysical areas that could not be spatially resolved with single optical telescopes (see Figures 2, 4, 6). The second generation of VLTI instruments has inherited and profited from the lessons learned, and the VLTI upgrade started in 2015 is providing a further enhanced facility (Woillez et al., 2015). The performance demonstrated today by GRAVITY shows that the initial goals set by AMBER were not unrealistic.

Part of AMBER's legacy is the novel way in which interferometric observables are extracted from the data, how fringe patterns are initially recorded. Another innovation is the pixel-to-visibility matrix

(P2VM) method implemented in the instrument's design. Originally invented for AMBER, this method has found its way into PIONIER and GRAVITY instruments.

Furthermore, AMBER was the first instrument for which real time fringe-tracking data were used to enhance the data reduction. This is routinely done for GRAVITY, and will likely be done for MATISSE. The latter instrument also inherited the fringe combination scheme employed by AMBER. Finally, the unique aspect of the AMBER instrument was its spectral resolution, which initiated the technique of spectro-interferometry. With a resolving power of 12 000, AMBER was able to spectrally and spatially resolve the dynamics of circumstellar phenomena, and paved the way for GRAVITY and MATISSE operations. The literature will no doubt continue to see numerous science papers originating from AMBER data in the coming years.

#### Acknowledgements

A large consortium of institutes, scientists and engineers contributed to AMBER. A list of the AMBER consortium members is included in this article<sup>1</sup>. We thank Armando Domiciano de Souza and Thomas Rivinius for useful discussions regarding classical Be stars.

#### References

Arroyo-Torres, B. et al. 2015, *A&A*, 575, 50  
 Baldwin, J. et al. 1996, *A&A*, 306, 13  
 Benisty, M. et al. 2010, *A&A*, 511, 75

Carciofi, A. et al. 2009, *A&A*, 504, 915  
 Chesneau, O. et al. 2007, *A&A*, 464, 119  
 Demory, B. O. et al. 2009, *A&A*, 505, 205  
 de Wit, W.-J. et al. 2014, *The Messenger*, 157, 50  
 Domiciano de Souza, M. et al. 2012, *A&A*, 545, 130  
 Gai, M. et al. 2004, *SPIE*, 5491, 528  
 Haguenaer, P. et al. 2008, *SPIE*, 7013, 7013C  
 Jennison, R. 1958, *MNRAS*, 118, 276  
 Kraus, S. et al. 2008, *A&A*, 489, 1157  
 Kraus, S. et al. 2010, *Nature*, 466, 339  
 Le Bouquin, J. B. et al. 2009, *A&A*, 496, L1  
 Le Bouquin, J. B. et al. 2009, *A&A*, 498, 41  
 Malbet, F. et al. 2007, *A&A*, 464, 43  
 Malbet, F. et al. 2008, arXiv:0808.1315  
 Meilland, A. et al. 2007, *A&A*, 464, 59  
 Mérand, A. et al. 2014, *SPIE*, 9146, 9146J  
 Ohnaka, K. et al. 2011, *A&A*, 529, 163  
 Ohnaka, K., Weigelt, G. & Hofmann, K.-H. 2017, *Nature*, 548, 310  
 Paresce, F. et al. 1996, *The Messenger*, 83, 14  
 Petrov, R. et al. 2007, *A&A*, 464, 1  
 Petrov, R. et al. 1998, *The Messenger*, 92, 11  
 Weigelt, G. et al. 2012, *A&A*, 541, L9  
 Weigelt, G. et al. 2016, *A&A*, 594, 106  
 Wittkowski, M. et al. 2008, *A&A*, 479, L21  
 Woillez, J. et al. 2015, *The Messenger*, 162, 16

#### Links

<sup>1</sup> List of AMBER consortium members:  
<http://amber.obs.ujf-grenoble.fr/spipe703.html>